ELSEVIER

Journal of Chromatography A, 853 (1999) 141–149

JOURNAL OF CHROMATOGRAPHY A

Interface for capillary electrophoresis coupled with inductively coupled plasma atomic emission spectrometry

Y.Y. Chan, W.T. Chan*

Department of Chemistry, University of Hong Kong, Pokfulam Road, Hong Kong, Hong Kong

Abstract

A modified concentric nebulizer was used as the interface to couple capillary electrophoresis (CE) to inductively coupled plasma atomic emission spectrometry (ICP-AES). The CE capillary replaces the central tube of the concentric nebulizer. The tip of the nebulizer tapers slowly to allow uncertainty in the position of the capillary. A platinum wire was inserted into the CE capillary to provide electrical connection to the CE power supply. pH changes inside the capillary due to electrolysis of the background buffer electrolyte was small and has minimal effects on the CE separation. The peak broadening effects due to the nebulizing gas flow, however, were significant. Resolution decreases quickly when the flow-rate of the carrier gas increases. Sample stacking technique was used to improve the resolution of species of opposite charge, e.g., Cr(VI) vs. Cr(III) ions. Detection limit of Cr based on peak area is ~10 ppb for the CE–ICP-AES system. © 1999 Elsevier Science B.V. All rights reserved.

Keywords: Interfaces; CE–ICP-AES; Capillary electrophoresis–inductively coupled plasma atomic emission spectrometry; Instrumentation; Chromium; Inorganic cations

1. Introduction

Capillary electrophoresis coupled to inductively coupled plasma atomic emission spectrometry (ICP-AES) and inductively coupled plasma mass spectrometry (ICP-MS) are powerful techniques for trace elemental speciation [1–19]. A challenge of the hybrid technique is the development of the CE–ICP interface. The CE–ICP interface should be compatible to the flow-rate of the CE and efficiently transform the CE effluent into aerosols for analyte transport to the ICP.

Typical setup of the CE–ICP-AES interface uses a nebulizer to convert the samples into fine aerosols. Various types of nebulizer, such as the conventional concentric nebulizer [1,2], micro-concentric nebulizer [3], direct injection nebulizer (DIN) [4], and ultrasonic nebulizer (USN) [5], have been used as the CE–ICP interface. The concentric nebulizer is most commonly used. An argon gas stream of high velocity draws the sample solution out of the concentric inner capillary and breaks the solution into fine aerosols. Typical solution uptake rate for a conventional concentric nebulizer, however, is 1–2 ml/min with 1% transport efficiency [20]. For the CE–ICP interface, the characteristics of the nebulizer must be modified to accommodate the CE solution flow-rate of μl/min or lower.

Another issue for the setup of the CE–ICP interface is the electrical connection of the outlet of the CE capillary to the CE power supply. The CE capillary is not dipped into a buffer vial as in the conventional CE setup. Therefore, the approach of a

*Corresponding author.
E-mail address: wtchan@hkusua.hku.hk (W.T. Chan)

0021-9673/99/$ – see front matter © 1999 Elsevier Science B.V. All rights reserved.
PII: S0021-9673(99)00713-X

Pt electrode in the buffer vial is not applicable. Several configurations have been described. A coaxial sheath flow of buffer round the CE capillary has been used to provide the electrical connection [2–19]. However, the CE analytes are diluted by the sheath flow. In addition, the liquid flow produces a pressure difference across the capillary and causes peak broadening. A different approach uses silver paint to coat the outside of the end section of the CE capillary [1]. No sheath flow of buffer is needed but contamination and deterioration of the silver paint is a concern.

In this paper, a simple CE–ICP interface is described. A locally-constructed nebulizer and spray chamber were used. The nebulizer was based on the conventional concentric nebulizer with the central capillary replaced by the CE capillary. The analytical performance of the interface was examined. Sample stacking technique was used for the separation of Cr(VI) and Cr(III) ions.

2. Experimental

2.1. Capillary electrophoresis

A commercial capillary electrophoresis instrument (Biofocus 2000 CE system, Bio-Rad Labs, Hercules, CA, USA) was used. The exit section of the CE capillary was placed inside the laboratory-made nebulizer (see the CE–ICP interface section). The exit of the CE capillary was held at a positive potential relative to the inlet; the potential difference across the capillary was 15 kV. Typical current during a CE run was ~15 μA.

The fused-silica CE capillary (Polymicro Technology, Phoenix, AZ, USA) has an internal diameter of 100 μm, external diameter of ~363 μm, and length of 1 m. For each run, sample length of approximately 15 cm was introduced into the capillary using hydrodynamic method: N_2 gas pressure=5 p.s.i., injection time=20 s (1 p.s.i.=6894.76 Pa). The argon nebulizing gas flow was stopped during sample injection.

2.2. Inductively coupled plasma–atomic emission spectrometer

An Echelle grating ICP-AES spectrometer (PlasmaQuant 110, Carl Zeiss, Jena, Germany) was used. The ICP forward power was 1.0 kW. The flow-rates of the intermediate and outer argon gas were 1 and 12 l/min, respectively. The flow-rate of the argon nebulizing gas was maintained at 0.87 l/min and monitored with a mass flow meter (FMA 1816, Omega Engineering, Stamford, CT, USA). The observation height was 10 mm above the coil. Temporal ICP emission intensity of Cr II 284.3 nm was measured at a sampling rate of 0.5 Hz over a CE run. Ar I 427.2 nm was used to check the spectrometer drift.

2.3. CE–ICP interface

A modified Meinhard concentric nebulizer was used as the CE–ICP interface (Fig. 1). The outer tube of the nebulizer is tapered much slower at the end compared to the conventional Meinhard nebulizer so that uncertainty in the position of the central capillary will not change the nebulizing efficiency drastically. The central tube of nebulizer is the fused-silica CE capillary. The end of the capillary was placed at 1 mm from the tip of the nebulizer. To fix the position of the CE capillary relative to the nebulizer, the CE capillary is threaded through a small hole that was punched on a septum (Puresep-T septa, diameter=6 mm and thickness=3 mm, Cole-Parmer, Vernon Hills, IL, USA). The septum was held at the end of the nebulizer with a PTFE reducer type connector (Union connector, reducer type, Cole-Parmer). One end of the PTFE connector (internal diameter 1.6 mm) was sealed by the septum and the other end (internal diameter 6 mm) was connected to the nebulizer.

A Pt wire (diameter=25 μm, length=10 cm) was used as the CE electrode. The end section (0.5 cm) of a Pt wire was inserted into the exit end of the CE capillary for electrical contact with the CE electrolyte. The other end of the platinum wire was threaded through the septum with the CE capillary and connected to the high voltage power supply of the CE instrument. The platinum wire was glued to the outside of the CE capillary with epoxy to fix its position relative to the CE capillary.

2.4. Chemical reagents

Stock solutions of 1000 ppm Cr(VI) and Cr(III)

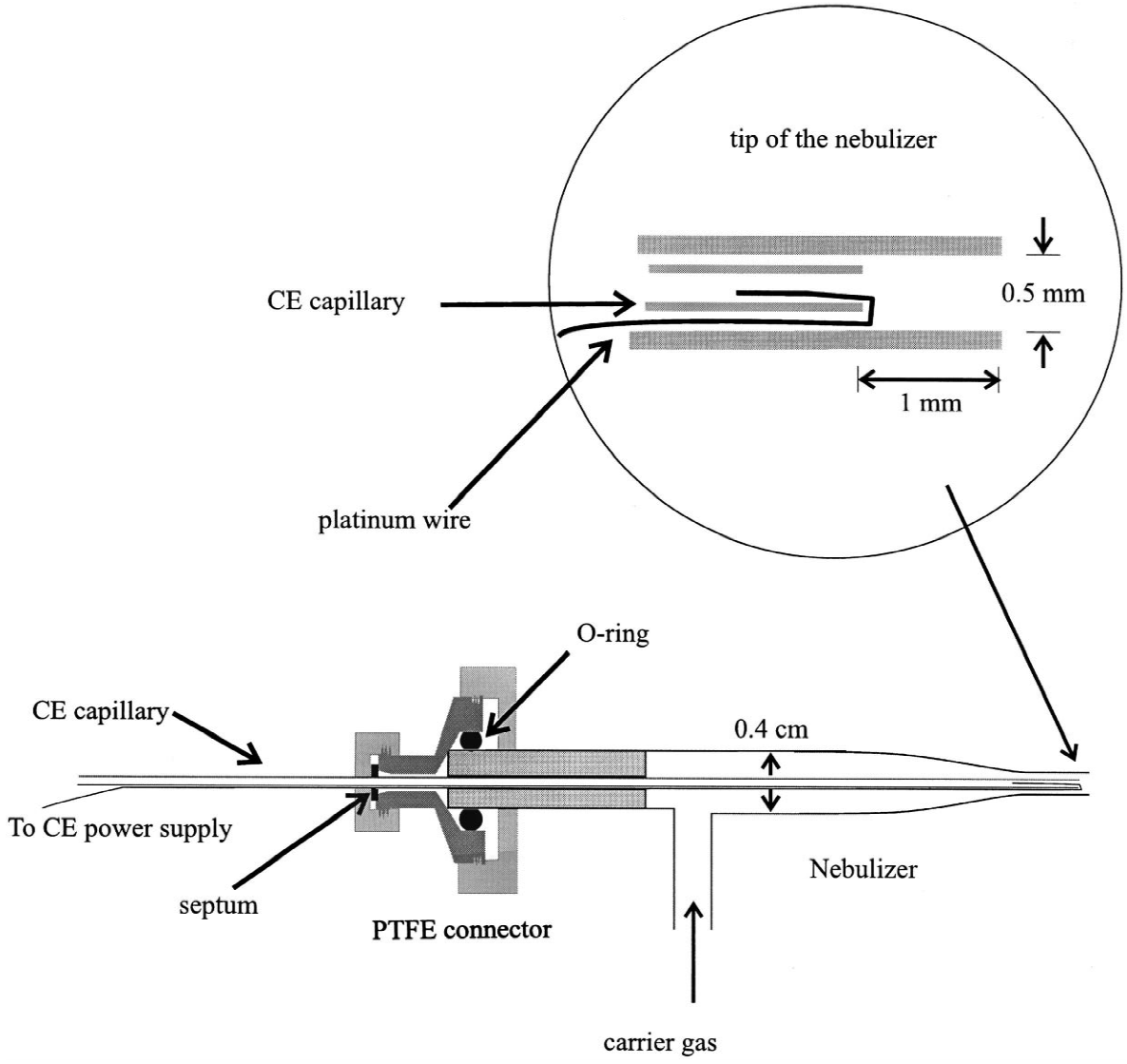

Fig. 1. Schematic diagram of the CE–ICP interface.

were prepared from $K_2Cr_2O_7$ (analytical reagent, Beijing Chemical Works, Beijing, China) and $CrCl_3 6H_2O$ (analytical-reagent grade, Aldrich, Milwaukee, WI, USA) in 1% nitric acid (guaranteed-reagent grade, Merck, Darmstadt, Germany). The two Cr stock solutions were mixed and diluted to 50 ppm with deionized water before the experiments. Sodium acetate buffer (0.02 *M*) was prepared from sodium acetate (analytical reagent grade, Beijing Chemical Works) and the pH of the buffer electrolyte was adjusted to 5.0 using diluted nitric acid.

3. Results and discussion

3.1. Effects of electrolysis at the counter electrode

Electrolysis of the background electrolyte occurs during capillary electrophoresis separation when a potential difference is applied across the CE electrodes [21–25]. The pH of the electrolyte near the electrode changes due to the removal of hydrogen or hydroxide ions. Since the pH of the CE electrolyte is a major parameter that influences the electroosmotic

flow (EOF) [22], the EOF flow-rate may change significantly and the direction of the EOF flow may even be reversed when there is a large change in pH.

Since sodium acetate was used as the buffer electrolyte, electrolysis of water occurred when the electric field was applied. For this CE–ICP setup, the anode was placed inside the CE capillary and was in contact with a small volume of the buffer solution ($\sim 2.67 \cdot 10^{-5}$ cm^3). If there is no solution flow, the change in pH will be large for the small volume of solution that is in contact with the platinum electrode.

To observe the pH change experimentally, the end of the capillary was placed under a microscope. A few drops of universal pH indicator were added to the CE buffer solution. The color of buffer near the electrode changed from pale pink to red in ~1 s when the electric field was applied. The large change in pH of the solution (from 5 to ~1) at the anode is due to the removal of hydroxide ions during electrolysis.

When a nebulizing gas flow was applied, the buffer solution was replenished continuously (gas flow-rate=0.58 l/min, solution flow-rate=$9.4 \cdot 10^{-5}$ ml/s; see next section). No color change of the universal pH indicator could be observed. Calculation based on acid-base equilibrium shows that, for a current of 15 μA, the pH change of the 0.02 *M* sodium acetate buffer solution is approximately 0.5. The pH changes during CE separation is relatively small and will not change the EOF flow-rate or the distribution of the species of the analyte significantly.

The inlet end of the capillary was fairly far away (approximately 2 mm apart) from the cathode. Also, the volume of the buffer solution in the vial was relatively large, ~2 ml. The pH change in the buffer vial is insignificant (ΔpH=0.04 for a typical CE run of 400 s) and will not effect the EOF during a normal CE run.

In addition to changes in pH, gas bubbles formed during electrolysis may block the electrical contact of the solution and the electrode. If there is no nebulizing gas flow, gas bubbles evolve at the surface of the anode, which can be observed under a microscope. The current drops from 15 μA to nearly zero within 2 sec upon the application of an electric field due to the gas bubble formation. If the nebulizer gas flow is applied, the solution is pulled out of the capillary via Bernoulli effect. The gas bubbles are removed from the capillary and the current stays steady during a CE run.

The length of the platinum wire inserted in the capillary is also critical. When a 1 mm long platinum wire was used, the current fluctuated because the small contact surface area can be obstructed by gas bubbles easily. A 5 mm long platinum wire was used in this study to provide a larger contact area.

3.2. Effect of nebulizing gas flow-rate on analyte migration time

The migration time (t_m) of CE–ICP separation of Cr(VI) and Cr(III) ions versus nebulizing gas flow-rate is shown in Fig. 2. When the carrier gas flow-rate increases, the pressure difference across the CE capillary increases. Therefore, the solution flow-rate increases and the migration time reduces.

In CE–ICP, the migration time (t_m) of an analyte is related to the electroosmotic flow-rate (V_{EOF}), the ionic mobilities (μ_i) of the analyte, and the flow-rate of the buffer solution (V_b) induced by the nebulizing gas flow (Fig. 3):

$$t_m = \frac{L_d}{V_{EOF} + V_b + \mu_i E} \quad (1)$$

where L_d is the length of the capillary and E is the applied electric field. The velocities are directional, i.e. they are treated as vectors during calculation.

The flow-rate of the buffer induced by the carrier gas flow (V_b) can be determined experimentally with the CE electric field turned off. The capillary was first filled with buffer solution. The free end of the capillary was then dipped into a sample vial containing 50 ppm of Cr(III) ions and the nebulizing gas flow was turned on. The ICP emission intensity against time was measured. An increase in Cr emission intensity indicates that the Cr solution has reached the nebulizer end of the capillary. V_b is equal to the total length of the capillary divided by the elution time. V_b versus carrier gas flow-rate is shown in Fig. 4.

The ionic mobility (μ_i) of the analyte is related to the ionic equivalent conductance λ_{equiv} (cm^2 $equiv^{-1}$ Ω^{-1}) [26]:

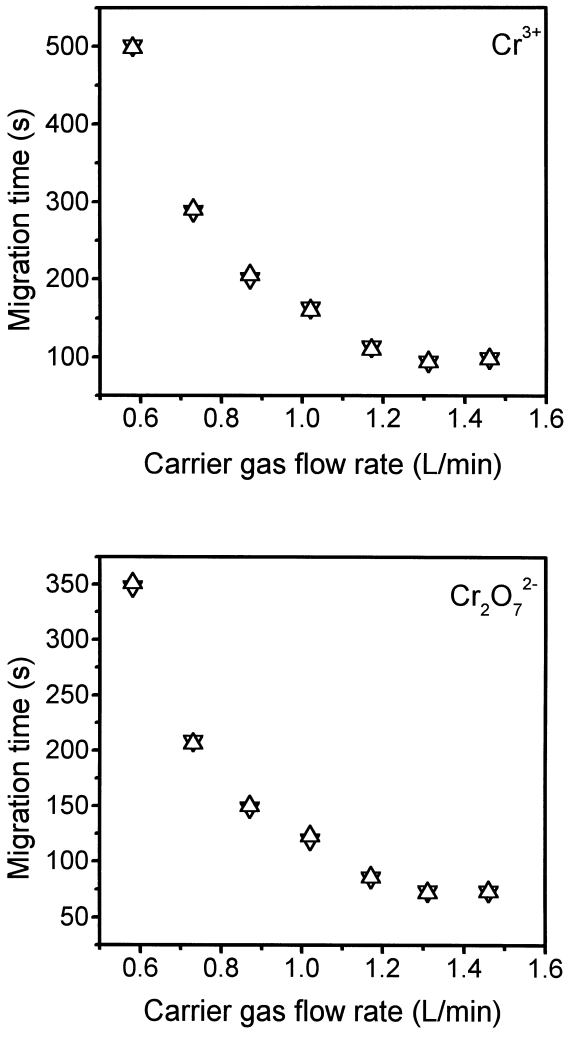

Fig. 2. Migration time of Cr(III) and Cr(VI) ions versus the flow-rate of carrier gas. (▽ and △ represent two independent runs.)

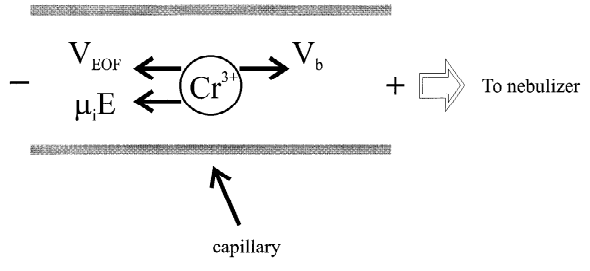

Fig. 3. Contribution of EOF, ionic mobility, and pneumatic flow to the migration of Cr(III) ion under an electric field.

$$\mu_i = \frac{\lambda_{equiv}}{F} \quad (2)$$

where F is the Faraday constant. For the Cr(III) ion, the equivalent ionic conductance is $67 \cdot 10^{-4}$ m^2 $equiv^{-1}$ Ω^{-1} [27]. The ionic mobility is $6.9 \cdot 10^{-4}$ cm^2 V^{-1} s^{-1}. For an applied electric field of 15 kV, the velocity of the ion under the electric field is approximately $1.0 \cdot 10^{-1}$ cm s^{-1}. The estimated ion velocity is probably higher than the actual velocity because limited equivalent ionic conductance was used in the calculation. Similarly, the equivalent ionic conductance of Cr(VI) ion is $85 \cdot 10^{-4}$ m^2 $equiv^{-1}\Omega^{-1}$ [27]; the ionic mobility is $8.8 \cdot 10^{-4}$ cm^2 V^{-1} s^{-1} and the velocity is $1.3 \cdot 10^{-1}$ cm s^{-1}.

Since μ_i, V_b and t_m are known, the electroosmotic flow-rate (V_{EOF}) can be calculated from Eq. (1). The magnitude of V_{EOF} is in the order of 10^{-2} cm s^{-1}. The magnitudes of V_b and V_{EOF} plus $\mu_i E$ for Cr(III) under different gas flow-rates are shown in Fig. 4. At carrier gas flow-rate of 0.6 L/min or below, the sum of V_{EOF} and $\mu_i E$ is of the same order of magnitude as V_b. When the gas flow increases to 1.45 L/min, V_b is 10 times of the sum of V_{EOF} and $\mu_i E$. The contribution of V_{EOF} and $\mu_i E$ to the analyte migration time is significant only at low nebulizing gas flow-rate. Since separation of ionic species by CE depends on μ_i and V_{EOF}, lower nebulizing gas flow-rate should be used to produce a smaller V_b and thus a longer migration time and better separation. Similarly, a longer and narrower CE capillary may also be used to reduce V_b.

3.3. Effect of nebulizing gas flow-rate on resolution

The electropherograms for the separation of Cr(VI) and Cr(III) ions with nebulizing gas flow-rate of 0.58, 0.87 and 1.45 l/min were shown in Fig. 5. The two peaks are completely separated at gas flow-rate of 0.58 l/min (Fig. 5a). At low gas flow-rate, the pressure difference across the CE capillary is small and the residence time of the ionic species is relatively long to allow separation of the species. As the gas flow-rate increases, the peaks begin to merge (Fig. 5b and c).

The resolution, R, of CE–ICP can be defined as [28]:

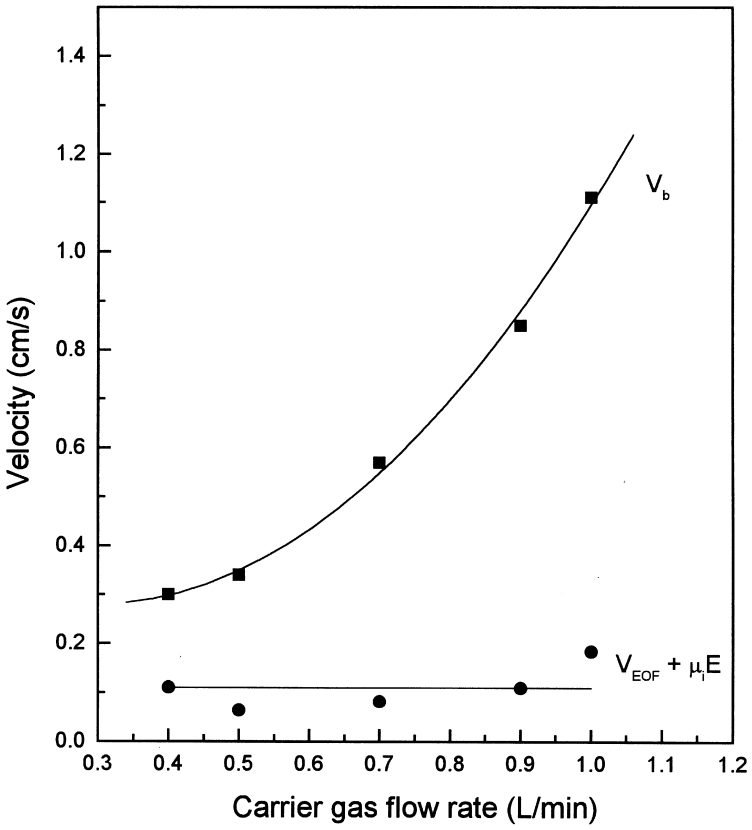

Fig. 4. Contributions of EOF, ionic mobility, and pneumatic flow to migration speed of Cr^{3+} versus carrier gas flow-rate (E field = 15 kV).

$$R = \frac{t_1 - t_2}{(\sigma_1 + \sigma_2)/2} \quad (3)$$

where t_1(s) and t_2 (s) are the migration times and σ_1 (s) and σ_2(s) are the full width at half maximum of Cr(III) and Cr(VI), respectively. The resolution for the two peaks at different nebulizing gas flow-rates is shown in Table 1. Resolution decreases as gas flow-rate increases.

The resolution for CE–ICP is related to the flow profile. In conventional CE, the major driving force of the solution flow is EOF that is generated by the movement of the bulk of water attached to the capillary wall. The flow profile is a flat top and will not introduce peak broadening [29]. In CE–ICP, however, a pressure difference was generated between the inlet and outlet of the capillary by the gas flow through the nebulizer opening. Since friction exists between the capillary and the buffer, a parabolic flow profile is formed [29]. The parabolic flow profile is a major variable contributing to peak broadening. The peak broadening effect increases with carrier gas flow-rate. Therefore, the resolution decreases when flow-rate increases.

In addition, a high flow-rate of the nebulizing gas increases V_b (Fig. 4) and reduces the residence time of the analyte ions in the CE capillary. The ions have a shorter period of time under the influence of the E field and may not be well separated.

3.4. Effect of sample stacking on peak width and resolution

Since the concentration of Cr ions in the sample solution is relatively low and the formation of complexes of Cr(III) with OH^- and Cl^- further reduces the concentration of the ions, the conduc-

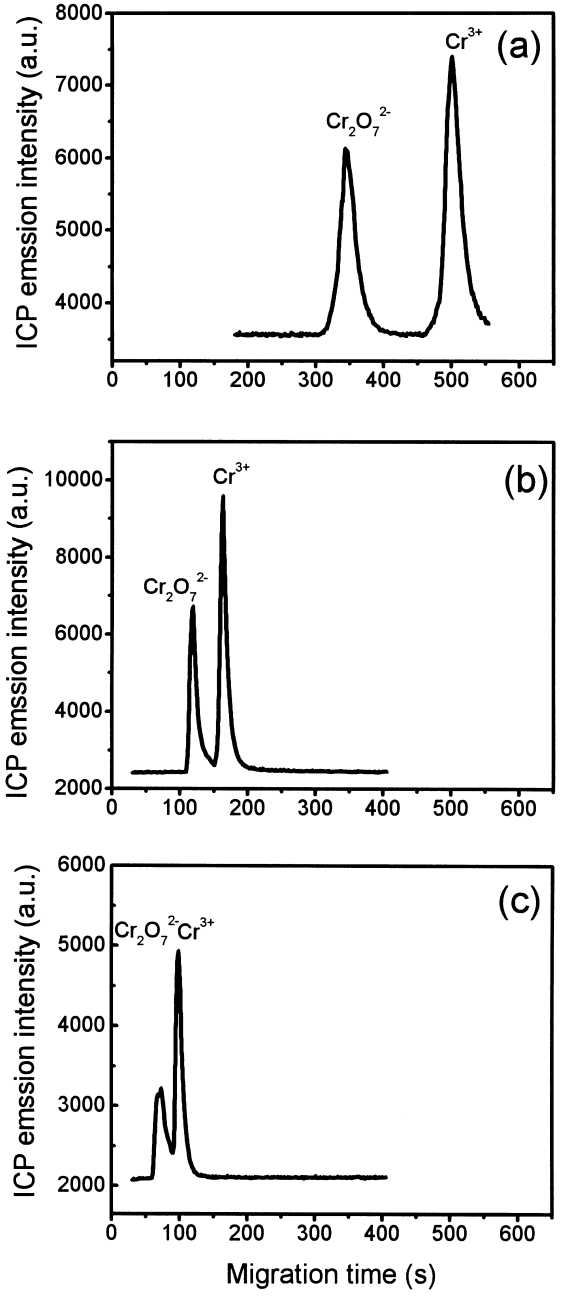

Fig. 5. Electropherograms for the separation of Cr(VI) and Cr(III) for nebulizing gas flow-rate of (a) 1.45 l/min, (b) 0.87 l/min, and (c) 0.58 l/min.

tivity of the Cr sample solution is smaller than that of the buffer solution. The difference in conductivity results in a larger E-field strength in the sample zone relative to the buffer zone. Sample stacking, therefore, may occur [30].

Table 1
Resolution of the Cr(VI) and Cr(III) peaks at different carrier gas flow-rate

Flow-rate (l/min)	Resolution
0.58	1.91
0.87	1.12
1.02	1.06
1.31	0.48
1.46	0.48

The field strength inside in the sample and buffer region can be estimated by the following equations [30]:

$$E_{\text{sample}} = \frac{\gamma E_o}{\gamma x + (1 - x)}$$
$$E_{\text{buffer}} = \frac{E_o}{\gamma x + (1 - x)} \quad (4)$$

where E_o is the average field strength, E_{sample} and E_{buffer} is the field strength of in the sample and buffer region, γ is the ratio of the specific conductance of the buffer to the sample region and x is the ratio of the sample length to the total length.

The CE–ICP-AES peak widths of Cr(VI) and Cr(III) versus sample length are shown in Fig. 6. The peak widths of both ions remain constant for sample lengths of 7 to 14 cm due to sample stacking. The peak widths of Cr(VI), however, increases quickly with sample length above 14 cm. The increase in peak width with sample length is probably due to the increase in the path length for the ions to migrate from one end of the sample zone to the other end and a reduction of E-field strength. From Eq. (4), the field strength in the sample decreases with sample length. When the length of the sample zone increases, the potential drop across the zone increases. However, the electric field is distributed over a longer length and the field strength reduces. Also, the elution time for the front of the sample zone decreases as sample length increases. The elution time of Cr(VI) ions is too short for complete stacking to occur. In contrast, the peak widths of Cr(III) remain approximately constant throughout the entire range of sample length studied. Since

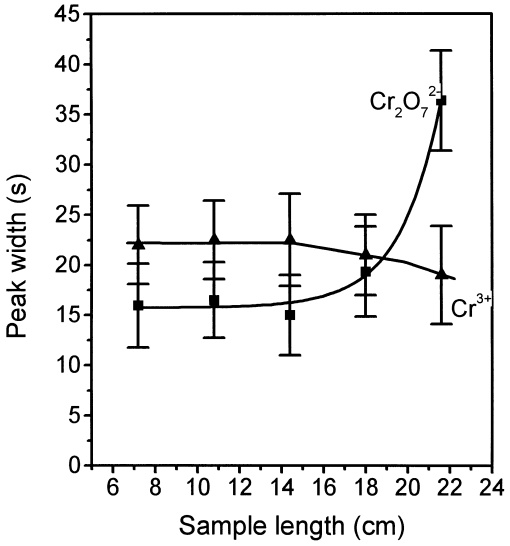

Fig. 6. Peak width of Cr(VI) and Cr(III) versus sample length.

Cr(III) and Cr(VI) ions migrate towards opposite directions, Cr(III) ions stay in the capillary for a longer period of time and stacking of the ions give a sharper CE–ICP-AES peak.

Resolution is related to the difference in migration time between the two peaks and the peak widths. The difference in migration time between the peaks increases as the sample length increases (Fig. 7). The curve rolls off when the sample length equals 14 cm

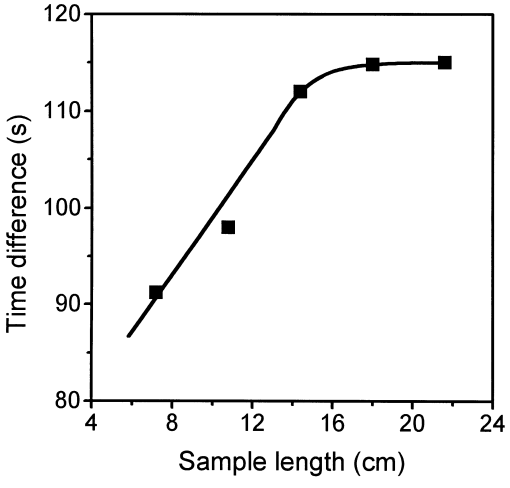

Fig. 7. Difference in migration time of Cr(VI) and Cr(III) versus sample length.

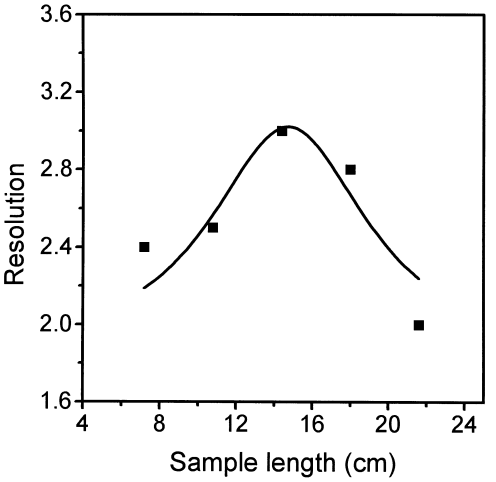

Fig. 8. Resolution of the Cr(VI) and Cr(III) peaks versus sample length.

or above due to a reduction in E-field strength and the elution time of Cr(VI) as discussed above.

The resolution for the Cr(VI) and Cr(III) peaks in CE–ICP separation against the sample length is shown in Fig. 8. Since the peak widths remain constant and the difference in migration time increases, the resolution increases when the sample length increases from 7 to 14 cm. The resolution of the two peaks, however, decreases when the sample length further increases above 14 cm because of the larger peak width of Cr(VI).

3.5. Calibration and detection limit

The linear dynamic range of Cr(VI) and Cr(III) for CE–ICP-AES is 1 to 100 ppm. The correlation coefficients for the calibration curves are 0.9957 and 0.9998, respectively.

The detection limit based on 3σ of the background intensity is 10 ppb for Cr, which is equivalent to $7.8 \cdot 10^{-12}$ g of Cr.

4. Conclusions

A simple CE–ICP interface based on a modified concentric nebulizer has been developed. A platinum wire electrode was inserted into the exit end of the CE capillary to complete the CE circuit. This ap-

proach ensures stable electrical contact between the electrode and the CE electrolyte. Furthermore, using a relatively small nebulizer orifice, a sheath flow is not needed in this setup for stable nebulization and CE operation. The solution flow-rate matches the V_{EOF} at low gas flow-rate. The carrier gas flow, however, introduces peak broadening. Low carrier gas flow-rate should be used for better CE–ICP resolution. Sample stacking technique has been used to improve resolution.

Acknowledgements

This paper was supported by CRCG grant of the University of Hong Kong.

References

[1] J.W. Olesik, J.A. Knitter, S.V. Olesik, Anal. Chem. 67 (1995) 1.
[2] Q. Lu, S.M. Bird, R.M. Barnes, Anal. Chem. 67 (1995) 2949.
[3] K.A. Taylor, B.L. Sharp, D.J. Lewis, H.M. Crews, J. Anal. At. Spectrom. 13 (1998) 1095.
[4] Y. Liu, V. Lopez-Avila, J.J. Zhu, D.R. Weiderin, W.F. Beckert, Anal. Chem. 67 (1995) 2020.
[5] Q. Lu, R.M. Barnes, Microchem. J. 54 (1996) 129.
[6] B. Michalke, P. Schramel, J. Chromatogr. A 750 (1996) 51.
[7] B. Michalke, S. Lustig, P. Schramel, Electrophoresis 18 (1997) 196.
[8] S.D. Lofthouse, G.M. Greenway, S.C. Stephen, J. Anal. At. Spectrom. 12 (1997) 1373.
[9] S. Lustig, B. Michalke, W. Beck, P. Schramel, Fresenius J. Anal. Chem. 360 (1998) 18.
[10] J.A. Kinzer, J.W. Olesik, S.V. Olesik, Anal. Chem. 68 (1996) 3250.
[11] E. Mei, H. Ichihashi, W. Gu, S. Yamasaki, Anal. Chem. 69 (1997) 2187.
[12] B. Michalke, P. Schramel, J. Chromatogr. A 807 (1998) 71.
[13] X.D. Tian, Z.X. Zhuang, B. Chen, X.R. Wang, Analyst 123 (1998) 899.
[14] V. Majidi, N.J. Miller-Ihli, Analyst 123 (1998) 803.
[15] B. Michalke, P. Schramel, Electrophoresis 19 (1998) 270.
[16] K.L. Sutton, C. B'Hymer, J.A. Caruso, J. Anal. At. Spectrom. 13 (1998) 885.
[17] M.L. Magnuson, J.T. Creed, C.A. Brockhoff, J. Anal. At. Spectrom. 12 (1997) 689.
[18] A. Tangen, R. Trones, T. Greibrokk, W. Lund, J. Anal. At. Spectrom. 12 (1997) 667.
[19] B. Michalke, P. Schramel, Fresenius J. Anal. Chem. 357 (1997) 594.
[20] M. Thompson, R.M. Barnes, in: A. Montaser, B.W. Golightly (Eds.), Inductively Coupled Plasma in Analytical Atomic Spectrometry, VCH, New York, 1992, Ch. 5.
[21] A. Vinther, H. Søeberg, J. Chromatogr. 589 (1992) 315.
[22] M. Macka, P. Andersson, P.R. Haddad, Anal. Chem. 70 (1998) 743.
[23] S. Carson, A.S. Cohen, A. Belenkii, M.C.R. Martinez, J. Berka, B.L. Karger, Anal. Chem. 65 (1993) 3219.
[24] M.A. Strege, A.L. Lagu, J. Liq. Chromatogr. 16 (1993) 51.
[25] M.S. Bello, J. Chromatogr. 744 (1996) 81.
[26] P. Jandik, G. Bonn, in: Capillary Electrophoresis of Small Molecules and Ions, VCH, New York, 1993, Ch. 2.
[27] D.R. Lide (Ed.), CRC Handbook of Chemistry and Physics, 78th ed., CRC Press, New York, 1997.
[28] R. Kuhn, S. Hoffstetter-Kuhn, Capillary Electrophoresis: Principle and Practice, Springer, New York, 1993, Ch. 2.6.
[29] D. Ishii, Introduction to Microscale High-Performance Liquid Chromatography, VCH, New York, 1988, Ch. 2.
[30] R. Kuhn, S. Hoffstetter-Kuhn, Capillary Electrophoresis: Principle and Practice, Springer, New York, 1993, Ch. 5.8.